Original Article

Nonlinear Dynamic Response and Vibration of 2D Penta-graphene Composite Plates Resting on Elastic Foundation in Thermal Environments

Nguyen Van Quyen[1], Vu Dinh Quang[1], Nguyen Dinh Duc[1,2,*], Pham Tien Lam[3,4]

[1] Department of Civil Engineering and Technology, VNU Hanoi University of Engineering and Technology (UET), 144 Xuan Thuy, Cau Giay, Hanoi, Vietnam

[2]Infrastructure Engineering Program, VNU Vietnam-Japan University (VJU),

My Dinh 1, Tu Liem, Hanoi, Vietnam

[3]PIAS, Phenikaa University, Yen Nghia, Hanoi, Vietnam

[4]JAIST, Asahidai 1-1, Nomi, Ishikawa, 923-1292, Japan

Abstract: This research discusses an analytical method for investigating vibration and dynamic response of plates structure made of 2-Dimensional (2D) penta-graphene. The density functional theory is used to figure out the elastic modulus of single layer penta-graphene. The classical plate theory is applied to determine basic equations of 2D penta-graphene composite plates. The numerical results are obtained by using the Bubnov-Galerkin method and Rung-Kutta method. The research results show high agreement in comparison with other studies. The results demonstrate the effect of shape parameters, material properties, foundation parameters and the mechanical load on the nonlinear dynamic response of 2D penta-graphene plates. The study also investigates the effect of the thermal environment on the behavior of 2D penta-graphene plates.

Keywords: Dynamic load, 2D penta-graphene composite plate, thermal environment, classical plate theory, stress function.

_____

*Corresponding author.
 Email address: ducnd@vnu.edu.vn

1. Introduction

Graphene like one 2D allotrope of carbon was have been known in 2004 [1]. It has shown that 2D single-layer structure has many outstanding advantages. Hence, scientists have been attracted considerable attention to these materials in the last decade. Computation or experimental methods have been used to investigate various types of 2D monolayer [2–7]. In 2015, Zhang et al. [8] proposed a new 2D carbon allotrope that is penta-graphene (PG). PG unit cell consists entirely of carbon pentagons.

As a highly stable 2D allotrope of carbon, scientists have been attracted to this material in recent years. In [9], Sun et al. investigated the thermal transport property of penta-graphene which is affected by grain boundaries. A highlight point in [10] shown that the thermal conductivity of graphene is higher than that of penta-graphene. Tien et al. [11] studied the transport and electronic properties of sawtooth PG nanoribbons. Tien et al. figure out that the electronic and the transport properties of sawtooth PG nanoribbons can effectively modulate when doping by N and H. Alborznia et al. [12] examined the electronic and optical properties of 2D penta-graphene when this material is affected by vertical compressive strain using density functional theory. In [13], the effect of temperature on mechanical properties investigated using simulation method. The mechanical properties of penta-graphene were compared with pentaheptite, graphane, and graphene in [14]. The mechanical properties of penta-graphene when this material is rolled into penta-graphene nanotubes was examined by Chen et al. [15]. Previous studies mainly focus on the material properties of penta-graphene. We can see that the number of studies on 2D penta-graphene application in the field of structure is still limited. Thus, this research decided to investigate the composite plate structure which reinforced by 2D penta-graphene.

The structures, in reality, face various types of dynamic loads such as wind, wave, earthquake, vehicle, blast, etc. Therefore, it is necessary to study the behavior of structures subjected to dynamic loads. Zhang et al. [16] use analytical and numerical methods to analyse the effect of blast loading on the behavior of plate structure which has three layers with faces made from fiber-metal and core made from metal foam. Blast loading effect on the dynamic response of plate structures with two layers sandwich was investigated [17]. Song et al. [18] studied the effect of moving to load on the dynamic response of sandwich plates base on the first-order shear deformation theory. In [19], Duc et al. presented nonlinear dynamic response and vibration of plate. The plate made from functionally material with piezoelectric layer, and outside stiffeners. In [20], dynamic response and vibration of double-curved shells which made from functionally graded nanocomposite have been studied base on higher-order shear deformation theory. Li et al. [21] investigated the nonlinear dynamic response sheet with triple-layer. The behavior of the composite plate reinforced by CNT under impact loading was studied using analytical method [22]. There are many studies on the behavior of structure when subjected to dynamic loads. But the number of research on structures made from 2D penta-graphene has not been paid attention to far. So this study decided to carry out the investigation Nonlinear dynamic response and vibration of 2D penta-graphene composite plates resting on elastic foundation in thermal environments.

2. Analytical solution

2.1. Basic formulas

Figure 1 shown the 2D penta-graphene composite plate model in the Cartesian coordinate system x, y, z on Pasternak foundation.

With xy is the mid-plane of the plates. z is the axis along with the thickness of the plate, ($-h/2 \leq z \leq h/2$). h is the thickness of the plate. a,b are the length and width of the plate, respectively.
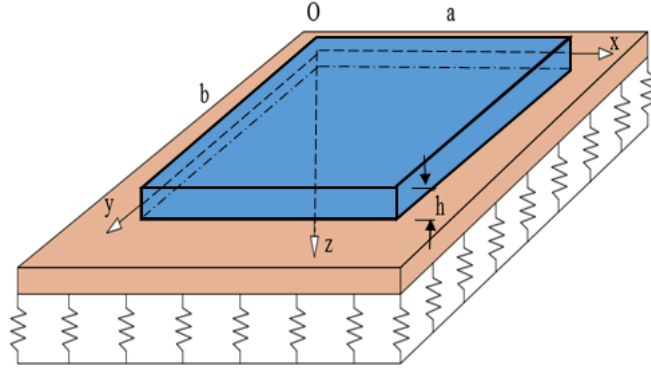
Figure 1. Geometry and coordinate system of the plate resting on Winkler and Pasternak foundations.

The reaction–deflection relation of the elastic foundation is expressed in Eq. (1):

$$q_e = k_1 w - k_2 \nabla^2 w \tag{1}$$

with $\nabla^2 = \dfrac{\partial^2}{\partial x^2} + \dfrac{\partial^2}{\partial y^2}$. w is the deflection of the plate. k_2 and k_1 are stiffness of Pasternak foundation and Winkler foundation, respectively.

The classical plate theory is used to build the compatibility, motions equations and examine the nonlinear dynamic response of the 2D penta-graphene composite plates in this research.

The relation strain-displacement base on classical plate theory is:

$$\begin{pmatrix} \varepsilon_x \\ \varepsilon_y \\ \gamma_{xy} \end{pmatrix} = \begin{pmatrix} \varepsilon_x^0 \\ \varepsilon_y^0 \\ \gamma_{xy}^0 \end{pmatrix} + z \begin{pmatrix} k_x \\ k_y \\ k_{xy} \end{pmatrix}, \tag{2}$$

with

$$\begin{pmatrix} \varepsilon_x^0 \\ \varepsilon_y^0 \\ \gamma_{xy}^0 \end{pmatrix} = \begin{pmatrix} u_{,x} + w_{,x}^2/2 \\ v_{,y} + w_{,y}^2/2 \\ u_{,y} + v_{,x} + w_{,x} w_{,y} \end{pmatrix},$$

$$\begin{pmatrix} k_x \\ k_y \\ k_{xy} \end{pmatrix} = \begin{pmatrix} -w_{,xx} \\ -w_{,yy} \\ -2w_{,xy} \end{pmatrix}, \tag{3}$$

in which the normal strains in the middle plane of the plate are ε_x^0 and ε_y^0 . The shear strain of the plate is γ_{xy}^0 inthemiddle plane of theplate. The displacement long x, y and z axes are u, v, w, respectively. k_x, k_y, k_{xy} are the curvature and twisted of the plates.

The relationship between stress and strain in the thermal environment is expressed through Hooke's law in Eq. (4)

$$\begin{pmatrix} \sigma_x \\ \sigma_y \\ \sigma_{xy} \end{pmatrix} = \begin{pmatrix} Q_{11} & Q_{12} & 0 \\ Q_{12} & Q_{22} & 0 \\ 0 & 0 & Q_{66} \end{pmatrix} \begin{pmatrix} \varepsilon_x - \alpha_1 \Delta T \\ \varepsilon_y - \alpha_2 \Delta T \\ \gamma_{xy} \end{pmatrix}, \tag{4}$$

With $\quad Q_{11} = \dfrac{E_{11}}{1 - \dfrac{E_{22}}{E_{11}} v_{12}^2} = \dfrac{E_{11}}{1 - v_{12} v_{21}}, Q_{22} = \dfrac{E_{22}}{1 - \dfrac{E_{22}}{E_{11}} v_{12}^2} = \dfrac{E_{22}}{E_{11}} Q_{11}, \ Q_{12} = v_{12} Q_{22}, Q_{66} = G_{12}.$

The elastic modulus of 2D penta-graphene obtained by fit the strain energy equation and the density functional theory energies.

The relationship between forces, moments and stress of the penta-graphene plates are given by Eq. (5)

$$\left(N_i, M_i \right) = \int_{-h/2}^{h/2} \sigma_i \left(1, z \right) dz, i = x, y, xy. \tag{5}$$

Substituting Eqs. (2) into Eqs. (4) and the result into Eqs. (5) give the constitutive relations as

$$\begin{aligned}
N_x &= A_{11}\varepsilon_x^0 + B_{11}k_x + A_{12}\varepsilon_y^0 + B_{12}k_y + A_{16}\gamma_{xy}^0 + B_{16}k_{xy} - \Delta T(\alpha_1 A_{11} + \alpha_2 A_{12}), \\
N_y &= A_{12}\varepsilon_x^0 + B_{12}k_x + A_{22}\varepsilon_y^0 + B_{22}k_y + A_{26}\gamma_{xy}^0 + B_{26}k_{xy} - \Delta T(\alpha_1 A_{12} + \alpha_2 A_{22}), \\
N_{xy} &= A_{16}\varepsilon_x^0 + B_{16}k_x + A_{26}\varepsilon_y^0 + B_{26}k_y + A_{66}\gamma_{xy}^0 + B_{66}k_{xy} - \Delta T(\alpha_1 A_{16} + \alpha_2 A_{26}), \\
M_x &= B_{11}\varepsilon_x^0 + D_{11}k_x + B_{12}\varepsilon_y^0 + D_{12}k_y + B_{16}\gamma_{xy}^0 + D_{16}k_{xy} - \Delta T(\alpha_1 B_{11} + \alpha_2 B_{12}), \\
M_y &= B_{12}\varepsilon_x^0 + D_{12}k_x + B_{22}\varepsilon_y^0 + D_{22}k_y + B_{26}\gamma_{xy}^0 + D_{26}k_{xy} - \Delta T(\alpha_1 B_{12} + \alpha_2 B_{22}), \\
M_{xy} &= B_{16}\varepsilon_x^0 + D_{16}k_x + B_{26}\varepsilon_y^0 + D_{26}k_y + B_{66}\gamma_{xy}^0 + D_{66}k_{xy} - \Delta T(\alpha_1 B_{16} + \alpha_2 B_{26}),
\end{aligned} \tag{6}$$

where

$$\begin{aligned}
A_{ij} &= \int_{-h/2}^{h/2} Q_{ij}(z)dz, & ij &= 11, 12, 16, \ 22, \ 26, 66. \\
B_{ij} &= \int_{-h/2}^{h/2} Q_{ij}(z)z\,dz, & ij &= 11, 12, 16, \ 22, \ 26, 66. \\
D_{ij} &= \int_{-h/2}^{h/2} Q_{ij}(z)z^2 dz. & ij &= 11, 22, 12, 66.
\end{aligned} \tag{7}$$

The motion equations of plates supported by elastic foundations base on classical plate theory are

$$N_{x,x} + N_{xy,y} = 0 \tag{8a}$$

$$N_{xy,x} + N_{y,y} = 0 \tag{8b}$$

$$M_{x,xx} + 2M_{xy,xy} + M_{y,yy} + N_x w_{,xx} + 2N_{xy} w_{,xy} + N_y w_{,yy} + q - k_1 w + k_2 \nabla^2 w = \rho_1 \frac{\partial^2 w}{\partial t^2} \tag{8c}$$

where q is an external pressure uniformly distributed on the surface of the plate and

$$\rho_1 = \int_{-h/2}^{h/2} \rho \, dz. \tag{9}$$

The stress function $f(x, y, t)$ is established as

$$N_x = \frac{\partial^2 f}{\partial y^2}, N_y = \frac{\partial^2 f}{\partial x^2}, N_{xy} = -\frac{\partial^2 f}{\partial x \partial y}. \tag{10}$$

From Eqs. (6), we get $\varepsilon_x^0, \varepsilon_y^0, \gamma_{xy}^0$ as follows

$$\varepsilon_x^0 = A_{11}^* N_x + A_{12}^* N_y + A_{16}^* N_{xy} - B_{11}^* k_x - B_{12}^* k_y - B_{16}^* k_{xy} + \Delta T (\alpha_1 D_{11}^* + \alpha_2 D_{12}^*),$$

$$\varepsilon_y^0 = A_{12}^* N_x + A_{22}^* N_y + A_{26}^* N_{xy} - B_{21}^* k_x - B_{22}^* k_y - B_{26}^* k_{xy} + \Delta T (\alpha_1 D_{21}^* + \alpha_2 D_{22}^*), \tag{11}$$

$$\varepsilon_{xy}^0 = A_{16}^* N_x + A_{26}^* N_y + A_{66}^* N_{xy} - B_{16}^* k_x - B_{26}^* k_y - B_{66}^* k_{xy} + \Delta T (\alpha_1 D_{16}^* + \alpha_2 D_{26}^*),$$

In which the coefficients $A_{ij}^*, B_{ij}^*, D_{ij}^*$ are explained in the Appendix.

With the stress function as in Eq. (10), Eqs. (8a-8b) are always satisfied. By substituting Eq. (11) into moment equations in Eq. (6). Finally, use the obtained moment equations instead of M_{ij} in Eq. (8c). After reduction, Eq. (8c) has the following form

$$P_1 f_{,xxxx} + P_2 f_{,yyyy} + P_3 w_{,xxyy} + P_4 w_{,xxxy} + P_5 w_{,xyyy} + P_6 w_{,xxxx} + P_7 w_{,yyyy} + P_8 w_{,xxyy}$$

$$+ P_9 w_{,xxxy} + P_{10} w_{,xyyy} + N_x w_{,xx} + 2N_{xy} w_{,xy} + N_y w_{,yy} + q - k_1 w + k_2 \nabla^2 w = \rho_1 \frac{\partial^2 w}{\partial t^2}, \tag{12}$$

In which the coefficients P_i (i =1-10) are given in the Appendix.

In this study, the imperfection is also considered. The equation to show the imperfections of the plate is w^*. From Eq. (12) for the perfect plate, we obtain Eq. (13) for imperfect plates.

$$P_1 f_{,xxxx} + P_2 f_{,yyyy} + P_3 w_{,xxyy} + P_4 w_{,xxxy} + P_5 w_{,xyyy} + P_6 w_{,xxxx} + P_7 w_{,yyyy} + P_8 w_{,xxyy}$$

$$+ P_9 w_{,xxxy} + + P_{10} w_{,xyyy} + f_{,yy}\left(w_{,xx} + w_{,xx}^*\right) - 2f_{,xy}\left(w_{,xy} + w_{,xy}^*\right) + f_{,xx}\left(w_{,yy} + w_{,yy}^*\right) \tag{13}$$

$$+ q - k_1 w + k_2 \nabla^2 w = \rho_1 \frac{\partial^2 w}{\partial t^2}.$$

The deformation compatibility equation of the perfect plates and imperfect plates are Eq. (14) and Eq. (15), respectively.

$$\varepsilon_{x,yy}^0 + \varepsilon_{y,xx}^0 - \gamma_{xy,xy}^0 = w_{,xy}^2 - w_{,xx} w_{,yy} \tag{14}$$

$$\varepsilon_{x,yy}^0 + \varepsilon_{y,xx}^0 - \gamma_{xy,xy}^0 = w_{,xy}^2 - w_{,xx}w_{,yy} + 2w_{,xy}w_{,xy}^* - w_{,xx}w_{,yy}^* - w_{,yy}w_{,xx}^* \tag{15}$$

Substitution Eq. (10) and Eq. (11) into the deformation compatibility Eq. (15) leads to

$$A_{22}^* f_{,xxxx} + E_1 f_{,xxyy} + A_{11}^* f_{,yyyy} - 2A_{26}^* f_{,xxxy} - 2A_{16}^* f_{,xyyy} + B_{21}^* w_{,xxxx} + B_{12}^* w_{,yyyy}$$
$$+ E_2 w_{,xxyy} + E_3 w_{,xxxy} + E_4 w_{,xyyy} - \left(w_{,xy}^2 - w_{,xx}w_{,yy} + 2w_{,xy}w_{,xy}^* - w_{,xx}w_{,yy}^* - w_{,yy}w_{,xx}^* \right) = 0, \tag{16}$$

In which E_i ($i = 1$-4) are given in the Appendix.

The Eq. (13) and Eq. (16) accompany with initial conditions and boundary conditions are used to investigate the nonlinear dynamic response of 2D penta-graphene plates.

2.2. Boundary conditions

In this study, the 2D penta-graphene composite plate is assumed to be simply supported. Two boundary conditions, labeled as Case I and Case II are considered

Case I. Four edges of the plate are simply supported and freely movable (FM)

$$w = N_{xy} = M_x = 0, N_x = N_{x0} \ \ at \ \ x = 0, a,$$
$$w = N_{xy} = M_y = 0, N_y = N_{y0} \ \ at \ \ y = 0, b. \tag{17}$$

Case II. Four edges of the plate are simply supported and immovable (IM)

$$w = u = M_x = 0, N_x = N_{x0} \ \ at \ \ x = 0, a,$$
$$w = v = M_y = 0, N_y = N_{y0} \ \ at \ \ y = 0, b. \tag{18}$$

in which N_{x0}, N_{y0} are compressive force along the direction x, y, respectively.

The approximate solutions satisfying the boundary conditions are

$$\left(w, w^* \right) = \left(W, \mu h \right) \sin \lambda_m x \sin \delta_n y, \tag{19}$$

$$f = A_1 \cos 2\lambda_m x + A_2 \cos 2\delta_n y + A_3 \sin \lambda_m x \sin \delta_n y + A_4 \cos \lambda_m x \cos \delta_n y + \frac{1}{2} N_{x0} y^2 + \frac{1}{2} N_{y0} x^2 \tag{20}$$

with $\lambda_m = \dfrac{m\pi}{a}, \beta_n = \dfrac{n\pi}{b}$, W - the amplitudes of the deflection of the plate. μ - imperfect parameter. The coefficients A_i ($i = 1 \div 4$) found are as follow

$$A_1 = \frac{1}{32A_{22}^*} \frac{\delta_n^2}{\lambda_m^2} W(W + 2\mu h),$$

$$A_2 = \frac{1}{32A_{11}^*} \frac{\lambda_m^2}{\delta_n^2} W(W + 2\mu h),$$

$$A_3 = \frac{(F_2 F_4 - F_1 F_3)}{F_2^2 - F_1^2} W, \tag{21}$$

$$A_4 = \frac{(F_2 F_3 - F_1 F_4)}{F_2^2 - F_1^2} W,$$

With F_i ($i = 1 \div 4$) are given in the Appendix.

Replacing Eq. (21), Eq. (20) and Eq. (19) into the Eq. (13) and then using Galerkin method we obtain Eq. (22)

$$
\frac{ab}{4}[P_1 \frac{(F_2F_4 - F_1F_3)}{F_2^2 - F_1^2}\lambda_m^4 + P_2 \frac{(F_2F_4 - F_1F_3)}{F_2^2 - F_1^2}\delta_n^4 + P_3 \frac{(F_2F_4 - F_1F_3)}{F_2^2 - F_1^2}\lambda_m^2\delta_n^2
$$

$$
-P_4 \frac{(F_2F_3 - F_1F_4)}{F_2^2 - F_1^2} - P_5 \frac{(F_2F_3 - F_1F_4)}{F_2^2 - F_1^2} + P_6\lambda_m^4 + P_7\delta_n^4 + P_8 \lambda_m^2\delta_n^2 - k_1 - k_2(\lambda_m^2 + \delta_n^2)]W
$$

$$
+\left[\frac{1}{3}\lambda_m\delta_n\left(P_1\frac{1}{A_{22}^*} + P_2\frac{1}{A_{11}^*}\right)\right]W(W + 2\mu h) + \frac{8}{3}\frac{(F_2F_4 - F_1F_3)}{F_2^2 - F_1^2}\lambda_m\delta_n W(W + \mu h) \qquad (22)
$$

$$
-\frac{ab}{64}\left(\frac{1}{A_{22}^*}\delta_n^4 + \frac{1}{A_{11}^*}\lambda_m^4\right)W(W + \mu h)(W + 2\mu h)
$$

$$
+\frac{ab}{4}\left(N_{x0}\lambda_m^2 + N_{y0}\delta_n^2\right)(W + \mu h) + \frac{4}{\lambda_m\delta_n}q = \rho_1 \frac{ab}{4}\frac{\partial^2 W}{\partial t^2}.
$$

2.3. Plates subjected to mechanical load

Consider the composite plates with Case I of boundary condition. The composite plates are assumed that subjected uniform compressive forces P_x and P_y (Pascal) on the edges $x = 0, a$, and $y = 0, b$

$$
N_{x0} = -P_xh, \ N_{y0} = -P_yh. \qquad (23)
$$

2.4. Plates with effect of temperature

Consider the composite plates with Case II ofboundary conditions in the thermal environment. The condition expressing the immovability on the edges, $u = 0$ (at $x = 0, a$) and $v = 0$ (at $y = 0, b$), is satisfied in an average sense as

$$
\int_0^b\int_0^a\frac{\partial u}{\partial x}dxdy = 0, \ \int_0^a\int_0^b\frac{\partial v}{\partial y}dxdy = 0. \qquad (24)
$$

From Eq. (3) and Eq. (14), we can obtain Eq. (25)

$$
\frac{\partial u}{\partial x} = A_{11}^*f_{,yy} + A_{12}^*f_{,xx} - A_{16}^*f_{,xy} + B_{11}^*w_{,xx} + B_{12}^*w_{,yy} + 2B_{16}^*w_{,xy}
$$

$$
+\Delta T(D_{11}^*\alpha_1 + D_{12}^*\alpha_2) - \frac{1}{2}w_{,x}^2 - w_{,x}w_{,x}^2
$$

$$
\qquad (25)
$$

$$
\frac{\partial v}{\partial y} = A_{12}^*f_{,yy} + A_{22}^*f_{,xx} - A_{26}^*f_{,xy} + B_{21}^*w_{,xx} + B_{22}^*w_{,yy} + 2B_{26}^*w_{,xy}
$$

$$
+\Delta T(D_{21}^*\alpha_1 + D_{22}^*\alpha_2) - \frac{1}{2}w_{,y}^2 - w_{,y}w_{,y}^2
$$

Substitution Eq. (19-20) into Eq. (25) and then results into Eq. (24), We can obtain the equation of N_{x0}, N_{y0} as below

$$N_{x0} = J_1 W + J_2 W(W + 2\mu h) + J_3 \Delta T$$
$$N_{y0} = J_4 W + J_5 W(W + 2\mu h) + J_6 \Delta T$$
(26)

where $J_i (i = 1 \div 6)$ are shown in the Appendix.

By substituting Eq. (26) into Eq. (22), leads to the basic equations used to investigate the nonlinear dynamic response of the 2D penta-graphene composite plates in the Case II of boundary condition

$$\frac{ab}{4}[P_1 \frac{(F_2 F_4 - F_1 F_3)}{F_2^2 - F_1^2} \lambda_m^4 + P_2 \frac{(F_2 F_4 - F_1 F_3)}{F_2^2 - F_1^2} \delta_n^4 + P_3 \frac{(F_2 F_4 - F_1 F_3)}{F_2^2 - F_1^2} \lambda_m^2 \delta_n^2$$

$$-P_4 \frac{(F_2 F_3 - F_1 F_4)}{F_2^2 - F_1^2} - P_5 \frac{(F_2 F_3 - F_1 F_4)}{F_2^2 - F_1^2} + P_6 \lambda_m^4 + P_7 \delta_n^4 + P_8 \lambda_m^2 \delta_n^2 - k_1 - k_2(\lambda_m^2 + \delta_n^2)]W$$

$$+\frac{ab}{4}(J_3 \Delta T \lambda_m^2 + J_6 \Delta T \delta_n^2)(W + \mu h) + \left[\frac{1}{3} \lambda_m \delta_n \left(P_1 \frac{1}{A_{22}^*} + P_2 \frac{1}{A_{11}^*}\right)\right] W(W + 2\mu h)$$

$$+\left[\frac{8}{3} \frac{(F_2 F_4 - F_1 F_3)}{F_2^2 - F_1^2} \lambda_m \delta_n + \frac{ab}{4}(J_1 \lambda_m^2 + J_4 \delta_n^2)\right] W(W + \mu h)$$
(27)

$$+\left[\frac{ab}{4}(J_2 \lambda_m^2 + J_5 \delta_n^2) - \frac{ab}{64}\left(\frac{1}{A_{22}^*} \delta_n^4 + \frac{1}{A_{11}^*} \lambda_m^4\right)\right] W(W + \mu h)(W + 2\mu h)$$

$$+\frac{4}{\lambda_m \delta_n} q = \rho_1 \frac{ab}{4} \frac{\partial^2 W}{\partial t^2}.$$

Eq. (27) is used to study behavior 2D penta-graphene composite plates subject dynamic load in the thermal environment on elastic foundation.

3. Numerical results and discussion

This research studied composite plates under the present of an exciting force $q = Q \sin \Omega t$. Q is the amplitude of exciting force and Ω is the frequency of the force. Numerical results for dynamic response and vibration of the composite plates are obtained by Runge–Kutta method.

We performed density functional theory calculations to estimate the elastic modulus of the single-layer penta-graphene. The structure of a penta-graphene sheet was derived from T12-carbon. Using fitting coefficients, we have estimated Q_{11} of 201.4 $GPa.nm$ and Q_{22} of 208.4 $GPa.nm$, Q_{12} of -18.6 $GPa.nm$ and the Q_{66} elastic constant was approximately 149.8 GPa, and thermal expansion coefficients of penta-graphene (α_1, α_2) are $(6.128, 6.128)$ 10^{-6}/K, respectively.

Table 1. The elastic of the 2D penta-graphene by our calculations

Q_{11}	Q_{22}	Q_{12}	Q_{66}	α_1	α_2
201.4	208.4	-18.6	149.8	6.128	6.128
$GPa.nm$	$GPa.nm$	$GPa.nm$	GPa	10^{-6}/K	10^{-6}/K

3.1. Validation

Park and Choi [23] studied the vibration of isotropic plates base on first-order shear deformation theory. In order to evaluate the accuracy of the method used in this research, we compared the value of the fundamental frequency parameter $\bar{\omega} = \omega_L a^2 \sqrt{\dfrac{\rho h}{D}}$ of plates in case of homogeneous plates without elastic foundations with results of Park and Choi [23].

Table 2 presents the influence of ratio length to thickness and ratio length to width on the fundamental frequency of the isotropic plates. From Table 2, the values of the fundamental frequencies obtained in this study very close to the results of Park and Choi [23]. The biggest difference is only 1.456%. This confirms that the method used in this study is completely reliable.

Table 2. Comparison of the fundamental natural frequencies $\bar{\omega} = \omega_L a^2 \sqrt{\dfrac{\rho h}{D}}$.

	b/a=0.5			b/a=1		
h/a	0.01	0.1	0.2	0.01	0.1	0.2
Park and Choi [23]	49.3045	45.5845	39.3847	19.7322	19.0840	17.5055
Present	49.1585	45.2167	38.9544	19.6127	18.8942	17.2507
Difference (%)	0.296	0.807	1.093	0.606	0.995	1.456

3.2. The natural frequency and dynamic response of 2D penta-graphene plates

Table 3. Effect of foundation and ratio b/a on natural frequencies $\left(s^{-1} \right)$ of 2D penta-graphene plates with ($\mu = 0, b/h = 100, (m,n) = (1,1)$)

(k_1, k_2)	b/a		
	1	1.5	2
(0.1, 0.02)	1629.0	1971.3	2368.9
(0.1, 0.04)	1697.9	2063.6	2486.9
(0.1, 0.06)	1764.1	2152.0	2599.6
(0.3, 0.02)	1985.9	2275.2	2627.1
(0.5, 0.02)	2287.8	2543.0	2862.2

Table 4. Effect of thickness and foundation on natural frequencies $\left(s^{-1} \right)$ of 2D penta-graphene plates with ($\mu = 0, b/a = 2$)

b/h	(k_1, k_2)	(m, n)			
		(1,1)	(1,3)	(1,5)	(3,5)
80	(0.1, 0.02)	1227.8	1711.0	2401.6	3353.4
	(0.3, 0.04)	1702.1	2115.8	2763.1	3708.0
	(0.5, 0.06)	2070.5	2454.7	3082.6	4031.6
90	(0.1, 0.02)	1151.7	1564.8	2166.2	3003.4
	(0.3, 0.04)	1641.8	1985.7	2537.5	3357.1
	(0.5, 0.06)	2016.0	2331.9	2861.0	3676.9
100	(0.1, 0.02)	1094.1	1451.1	1980.8	2725.7
	(0.3, 0.04)	1597.2	1887.2	2362.9	3081.6
	(0.5, 0.06)	1976.1	2240.0	2691.2	3400.5

Table 3 and Figure 2 show the effect of ratio length to width a/b on the behavior of 2D penta-graphene composite plate. Table 2 shows the natural frequencies of penta-graphene with three case ratio $b/a = (1, 1.5, 2)$. The natural frequencies of the plate increase significantly when the ratio of b/a increases. In case $(k_1, k_2) = (0.1, 0.02)$, respectively, the natural frequencies increase 45.4% when ratio b/a increase from 1 to 2. Figure 3 shows the dynamic response of penta-graphene plate with three cases of $b/a = (2, 2.5, 3)$. From Figure 3, it is noticeable that the amplitude of the fluctuation of the structure is larger when the ratio of b/a decreases.

Table 4 and Figure 3 present the effect of length to thickness b/h on the behavior of 2D penta-graphene composite plate. A glance at Table 4 provided reveals the effect of ratio b/h on natural frequencies of the penta-graphene plate. We considered three values of ratio $b/h = (80, 90, 100)$. It can see that natural oscillation frequency decrease when b/h increase. In case $(k_1, k_2) = (0.1, 0.02)$, respectively, the natural frequency decrease from 1227.8 (s^{-1}) to 1094.1 (s^{-1}) when b/h increase from 80 to 100. Figure 3 provided show the ratio length to thickness b/h affect the dynamic response of penta-graphene plate. Three case of ratio $b/h = (60, 80, 100)$. The value of the amplitude of the penta-graphene plates increases when the value of ratio b/h increase. When the plate is thick, the structure is stronger.
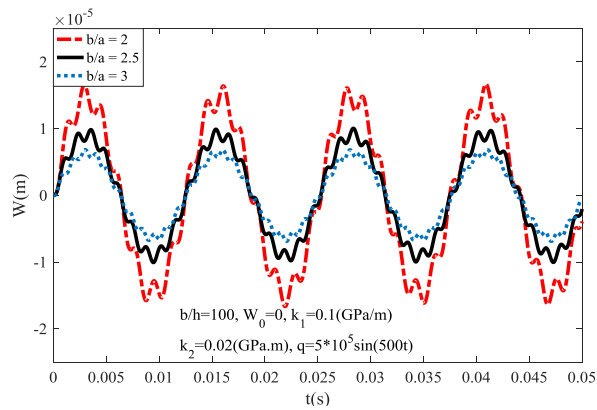
Figure 2. The ratio length to width a/b affect the behavior of the plate.
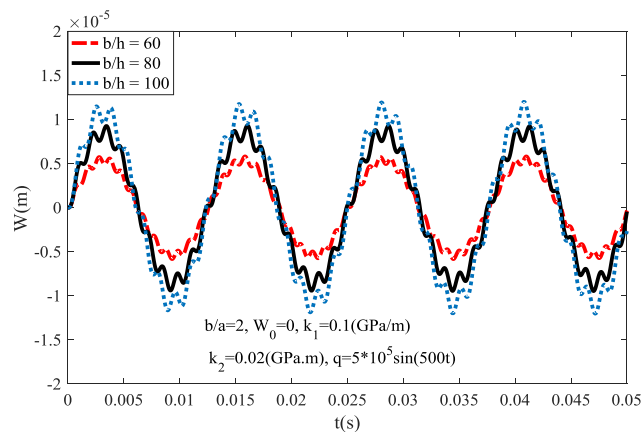
Figure 3. The ratio length to thickness b/h affect the behavior of the plate.

We can see the effect of the elastic foundation on the behavior of penta-graphene plate from Table 3, Table 4, Figure 4 and Figure 5. Table 3 and Table 4 present the influence of the elastic foundation on the natural frequency of the plate. From those two tables, the frequency of plate increases significantly when the stiffness of the elastic foundation increases. Figures 4 and 5 show the influence of the foundation on the dynamic response of penta-graphene plates. Figure 4 considered three values of $k_1 = (0.1, 0.5, 0.9)$ (GPa/m). Figure 5 considered three values of $k_2 = (0.02, 0.06, 0.1)$ (GPa.m). Elastic foundation especially Pasternak foundation has a positive effect on the dynamic response of penta-graphene plates. When the stiffness of the elastic foundation increases, the amplitude of the plate will decrease.
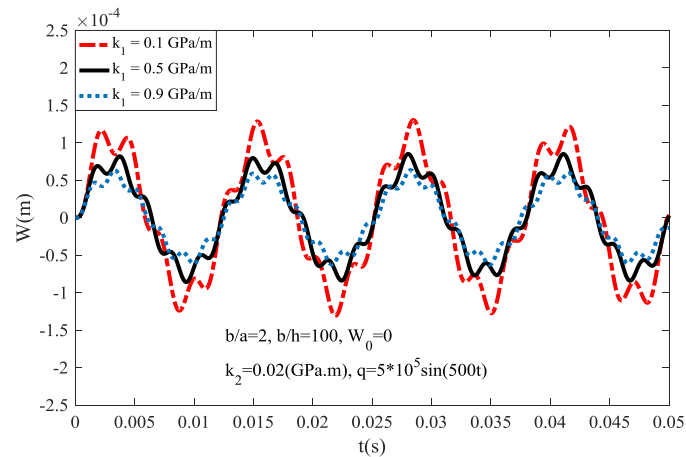
Figure 4. Winkler foundation k_1 affect the behavior of the plate.
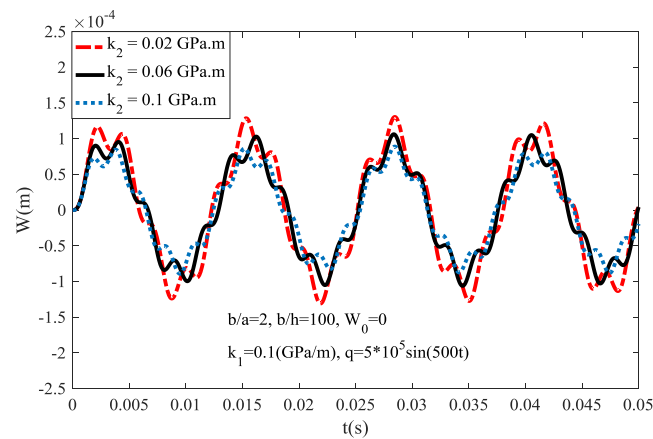
Figure 5. Pasternak foundation k_2 affect the behavior of the plate.

Figure 6 illustrates the impact of the initial imperfection of plate on the dynamic response of penta-graphene plate. Three case $\mu = (0, 0.1, 0.2)$ was investigated in Figure 6. The plate is perfect when $\mu = 0$. When the initial imperfect coefficient increase, the fluctuation range of the plate decreases.

Figure 7 demonstrates the impact of the thermal environment on the deflection amplitude – time curve of the plate. Three values $\Delta T = (900, 700, 500)$ were investigated in Figure 7. Obviously, the thermal environment has a negative effect on the nonlinear dynamic response of penta-graphene plate. The temperature of the environment causes the amplitude fluctuation of the plate to increase.
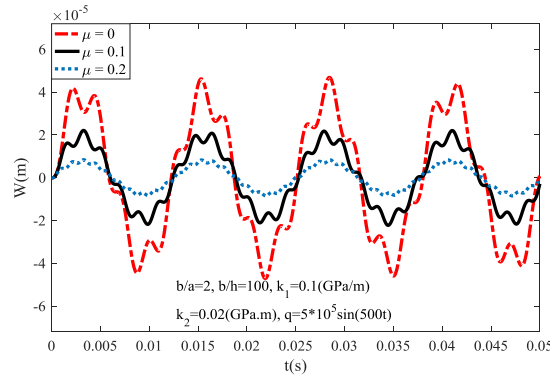
Figure 6. Imperfect coefficient μ affects the behavior of the plate.
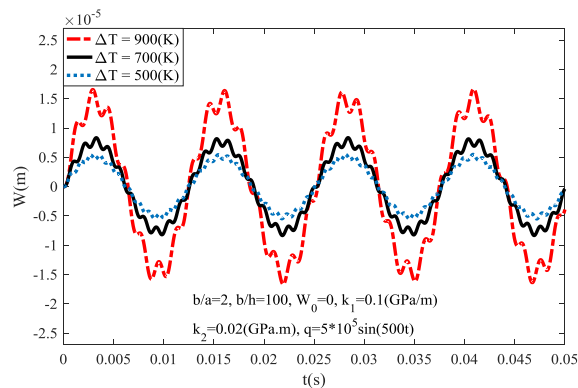
Figure 7. Thermal environment affects the behavior of the plate.

Figure 8 shows the effect of exciting force amplitude on the dynamic response of penta-graphene plates. In Figure 8, three cases of the excitation force amplitude $Q = \left(500\,kN\,/\,m^2, 400\,kN\,/\,m^2, 300\,kN\,/\,m^2\right)$ were considered. The amplitude of the excited force has a clear negative impact on the dynamic response of penta-graphene plate.

Figure 9 demonstrates the impact of pre-loaded axial compression P_x on the behavior of penta-graphene plates. From Figure 9, the value of the amplitude fluctuation of the plate to increase when the value of pre-loaded axial compression increase from 0 GPa to 0.6 GPa.

Figure 10 introduces the effect of the amplitude Q on the graph of the frequency and amplitude. Obviously, the frequency – amplitude curve in the middle of the frequency – amplitude curves of forced vibration. When the value of the amplitude Q increase, the frequency – amplitude curves of force vibration and free vibration are farther apart.
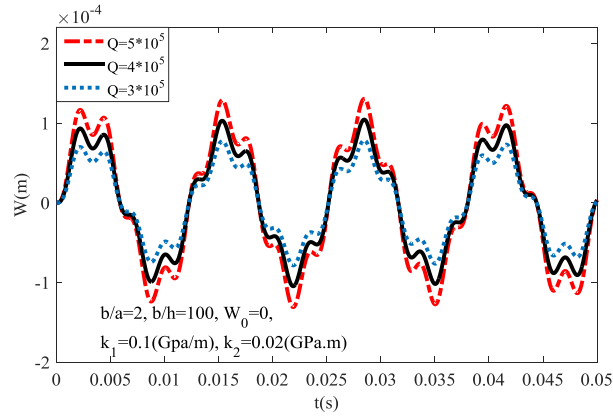
Figure 8. The amplitude Q affects the behavior of plate.
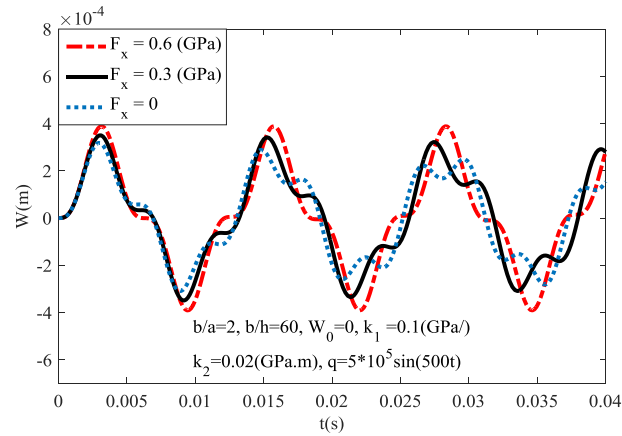
Figure 9. The pre-loaded axial P_x affect the behavior of plate.
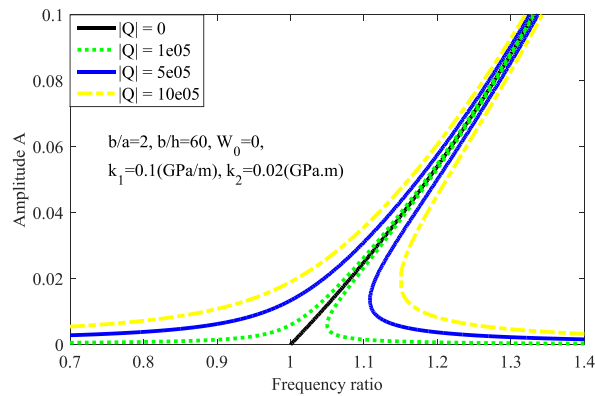
Figure 10. The amplitude Q affects the frequency – amplitude curves of plate

4. Conclusions

This research analysed the behavior of penta-graphene composite plates on elastic foundation based on the classical plate theory and Airy stress function. The elastic modulus of 2D penta-graphene obtained by fit the strain energy equation and the density functional theory energies.

One highlight in this study was the study of the effect of the thermal environment on the behavior of penta-graphene plate. From the results of the study, the conclusions obtained are:

- The value of the natural frequency of the penta-graphene plate affected by geometrical parameters and elastic foundations has been examined.

- The influences ofgeometrical parameters on the nonlinear dynamic response curves of the penta-graphene plate are examined.

- The elastic foundations have a positive effect while excitation force and mechanical loads have negative effect on the nonlinear dynamic response curves of the penta-graphene plates.

- The influence of temperature field on the nonlinear dynamic response curves of penta-graphene plates are investigated. Specifically, increasing temperature of the environment adversely affects the behavior of the penta-graphene plates.

Acknowledgment

References

[1] K.S. Novoselov, A.K. Geim, S.V.Morozov, D. Jiang, Y. Zhang, S.V. Dubonos, I.V. Grigorieva, A.A. Firsov, Electric field effect in atomically thin carbon films, Science 306 (2004) 666–669.

[2] M.E. Dávila, L. Xian, S. Cahangirov, A. Rubio, G. Le Lay, Germanene: a novel two-dimensional germanium allotrope akin to graphene and silicene, New J. Phys. 16 (2014) 95002.

[3] S. Balendhran, S. Walia, H. Nili, S. Sriram, M. Bhaskaran, Elemental analogues of graphene: silicene, germanene, stanene, and phosphorene, Small. 11 (2015) 640–652.

[4] P. Vogt, P. De Padova, C. Quaresima, J. Avila, E. Frantzeskakis, M.C. Asensio, A. Resta, B. Ealet, G. Le Lay, Silicene: compelling experimental evidence for graphenelike two-dimensional silicon, Phys. Rev. Lett. 108 (2012) 155501.

[5] S. Cahangirov, M. Topsakal, E. Aktürk, H. Şahin, S. Ciraci, Two-and one-dimensional honeycomb structures of silicon and germanium, Phys. Rev. Lett. 102 (2009) 236804.

[6] S. Zhang, Z. Yan, Y. Li, Z. Chen, H. Zeng, Atomically thin arsenene and antimonene: semimetal–semiconductor and indirect–direct band-gap transitions, Angew. Chemie Int. Ed. 54 (2015) 3112–3115.

[7] J. Ji, X. Song, J. Liu, Z. Yan, C. Huo, S. Zhang, M. Su, L. Liao, W. Wang, Z. Ni, Two-dimensional antimonene single crystals grown by van der Waals epitaxy, Nat. Commun. 7 (2016) 13352.

[8] Z. Shunhong, Z. Jian, W. Qian, C. Xiaoshuang, K. Yoshiyuki, J. Puru, Penta-graphene: A new carbon allotrope, Proceedings of the National Academy of Sciences. 112 (2015) 2372-2377.

[9] J. Sun, Y. Guo, Q. Wang, Y. Kawazoe, Thermal transport properties of penta-graphene with grain boundaries, Carbon N. Y. 145 (2019) 445–451.

[10] W. Xu, G. Zhang, B. Li, Thermal conductivity of penta-graphene from molecular dynamics study, J. Chem. Phys. 143 (2015) 154703.

[11] N.T. Tien, P.T.B. Thao, V.T. Phuc, R. Ahuja, Electronic and transport features of sawtooth penta-graphene nanoribbons via substitutional doping, Phys. E Low-Dimensional Syst. Nanostructures. 114 (2019) 113572.

[12] H. Alborznia, M. Naseri, N. Fatahi, Buckling strain effects on electronic and optical aspects of penta-graphene nanostructure, Superlattices Microstruct. (2019) 106217.

[13] M.-Q. Le, Mechanical properties of penta-graphene, hydrogenated penta-graphene, and penta-CN2 sheets, Comput. Mater. Sci. 136 (2017) 181–190.

[14] H. Sun, S. Mukherjee, C.V. Singh, Mechanical properties of monolayer penta-graphene and phagraphene: a first-principles study, Phys. Chem. Chem. Phys. 18 (2016) 26736–26742.

[15] M. Chen, H. Zhan, Y. Zhu, H. Wu, Y. Gu, Mechanical properties of penta-graphene nanotubes, J. Phys. Chem. C. 121 (2017) 9642–9647.

[16] J. Zhang, Y. Ye, Q. Qin, On dynamic response of rectangular sandwich plates with fibre-metal laminate face-sheets under blast loading, Thin-Walled Struct. 144 (2019) 106288

[17] J. Zhang, R. Zhou, M. Wang, Q. Qin, Y. Ye, T.J. Wang, Dynamic response of double-layer rectangular sandwich plates with metal foam cores subjected to blast loading, Int. J. Impact Eng. 122 (2018) 265–275.

[18] Q. Song, Z. Liu, J. Shi, Y. Wan, Parametric study of dynamic response of sandwich plate under moving loads, Thin-Walled Struct. 123 (2018) 82–99.

[19] N. D. Duc, P. H. Cong, Nonlinear thermo-mechanical dynamic analysis and vibration of higher order shear deformable piezoelectric functionally graded material sandwich plates resting on elastic foundations, J. Sandw. Struct. Mater. 20 (2016) 191–218.

[20] N.D. Duc, H. Hadavinia, T.Q. Quan, N.D. Khoa, Free vibration and nonlinear dynamic response of imperfect nanocomposite FG-CNTRC double curved shallow shells in thermal environment, Eur. J. Mech. - A/Solids. 75 (2019) 355–366.

[21] H.B. Li, X. Wang, J.B. Chen, Nonlinear dynamic responses of triple-layered graphene sheets under moving particles and an external magnetic field, Int. J. Mech. Sci. 136 (2018) 413–423.

[22] Z.G. Song, L.W. Zhang, K.M. Liew, Dynamic responses of CNT reinforced composite plates subjected to impact loading, Compos. Part B Eng. 99 (2016) 154–161.

[23] M. Park, D.-H. Choi, A two-variable first-order shear deformation theory considering in-plane rotation for bending, buckling and free vibration analyses of isotropic plates, Appl. Math. Model. 61 (2018) 49–71.

Appendix

$$A_{11}^* = \frac{A_{22}A_{66} - A_{26}^2}{\Delta}, A_{12}^* = \frac{A_{16}A_{26} - A_{12}A_{66}}{\Delta}, A_{16}^* = \frac{A_{12}A_{26} - A_{22}A_{16}}{\Delta},$$

$$A_{22}^* = \frac{A_{11}A_{66} - A_{16}^2}{\Delta}, A_{26}^* = \frac{A_{12}A_{16} - A_{11}A_{26}}{\Delta}, A_{66}^* = \frac{A_{11}A_{22} - A_{12}^2}{\Delta},$$

$$\Delta = A_{11}A_{22}A_{66} - A_{11}A_{26}^2 + 2A_{12}A_{16}A_{26} - A_{12}^2A_{66} - A_{16}^2A_{22},$$

$$B_{11}^* = A_{11}^*B_{11} + A_{12}^*B_{12} + A_{16}^*B_{16}, B_{12}^* = A_{11}^*B_{12} + A_{12}^*B_{22} + A_{16}^*B_{26},$$

$$B_{16}^* = A_{11}^*B_{16} + A_{12}^*B_{26} + A_{16}^*B_{66}, B_{21}^* = A_{12}^*B_{11} + A_{22}^*B_{12} + A_{26}^*B_{16},$$

$$B_{22}^* = A_{12}^*B_{12} + A_{22}^*B_{22} + A_{26}^*B_{26}, B_{26}^* = A_{12}^*B_{16} + A_{22}^*B_{26} + A_{26}^*B_{66},$$

$$B_{61}^* = A_{16}^*B_{11} + A_{26}^*B_{12} + A_{66}^*B_{16}, B_{62}^* = A_{16}^*B_{12} + A_{26}^*B_{22} + A_{66}^*B_{26},$$

$$B_{66}^* = A_{16}^*B_{16} + A_{26}^*B_{26} + A_{66}^*B_{66}, D_{11}^* = A_{12}^*A_{11} + A_{12}^*A_{12} + A_{16}^*A_{16},$$

$$D_{12}^* = A_{12}^*A_{12} + A_{22}^*A_{22} + A_{26}^*A_{26}, D_{21}^* = A_{12}^*A_{11} + A_{22}^*A_{12} + A_{26}^*A_{16},$$

$$D_{22}^* = A_{12}^*A_{12} + A_{22}^*A_{22} + A_{26}^*A_{26}, D_{16}^* = A_{16}^*A_{11} + A_{26}^*A_{12} + A_{66}^*A_{16},$$

$$D_{26}^* = A_{16}^*A_{12} + A_{26}^*A_{22} + A_{66}^*A_{26}$$

$$P_1 = B_{21}^*, P_2 = B_{12}^*, P_3 = B_{11}^* + B_{22}^* - 2B_{66}^*, P_4 = 2B_{26}^* - B_{61}^*,$$

$$P_5 = 2B_{16}^* - B_{62}^*, P_6 = B_{11}B_{11}^* + B_{12}B_{21}^* + B_{16}B_{61}^*, P_7 = B_{12}B_{12}^* + B_{22}B_{22}^* + B_{26}B_{62}^*,$$

$$P_8 = B_{11}B_{12}^* + B_{12}B_{22}^* + B_{16}B_{62}^* + B_{12}B_{11}^* + B_{22}B_{21}^* + B_{26}B_{61}^* + 4B_{16}B_{16}^* + 4B_{26}B_{26}^* + 4B_{66}B_{66}^*,$$

$$P_9 = 2(B_{11}B_{16}^* + B_{12}B_{26}^* + B_{16}B_{66}^* + B_{16}B_{11}^* + B_{26}B_{21}^* + B_{66}B_{61}^*),$$

$$P_{10} = 2(B_{12}B_{16}^* + B_{22}B_{26}^* + B_{26}B_{66}^* + B_{16}B_{12}^* + B_{26}B_{22}^* + B_{66}B_{62}^*).$$

$$E_1 = 2A_{12}^* + A_{66}^*, E_2 = B_{11}^* + B_{22}^* - 2B_{66}^*,$$

$$E_3 = 2B_{26}^* - B_{61}^*, E_4 = 2B_{16}^* + B_{62}^*.$$

$$F_1 = A_{22}^* \lambda_m^4 + A_{11}^* \delta_n^4 + E_1 \lambda_m^2 \delta_n^2,$$

$$F_2 = 2A_{26}^* \lambda_m^3 \delta_n + 2A_{16}^* \lambda_m \delta_n^3,$$

$$F_3 = -B_{21}^* \lambda_m^4 - B_{12}^* \delta_n^4 - E_2 \lambda_m^2 \delta_n^2,$$

$$F_4 = E_3 \lambda_m^3 \delta_n + E_4 \lambda_m \delta_n^3,$$

$$J_1 = \frac{A_{22}^* L_1 - A_{12}^* L_3}{A_{11}^* A_{22}^* - A_{12}^{*2}}, J_2 = \frac{A_{22}^* L_2 - A_{12}^* L_4}{A_{11}^* A_{22}^* - A_{12}^{*2}}, J_3 = -\frac{A_{22}^* H_1 - A_{12}^* H_2}{A_{11}^* A_{22}^* - A_{12}^{*2}},$$

$$J_4 = \frac{A_{11}^* L_3 - A_{12}^* L_1}{A_{11}^* A_{22}^* - A_{12}^{*2}}, J_5 = \frac{A_{11}^* L_4 - A_{12}^* L_2}{A_{11}^* A_{22}^* - A_{12}^{*2}}, J_6 = -\frac{A_{11}^* H_1 - A_{12}^* H_2}{A_{11}^* A_{22}^* - A_{12}^{*2}}$$

$$L_1 = \frac{1}{ab} \frac{(A_{11}^* \delta_n^2 + A_{12}^* \lambda_m^2)}{\lambda_m \delta_n} \frac{(Q_2 Q_4 - Q_1 Q_3)}{Q_2^2 - Q_1^2} + 4A_{16}^* \frac{(Q_2 Q_3 - Q_1 Q_4)}{Q_2^2 - Q_1^2} + 4(B_{11}^* \lambda_m^2 + B_{12}^* \delta_n^2)$$

$$L_3 = \frac{1}{ab} \frac{(A_{12}^* \delta_n^2 + A_{22}^* \lambda_m^2)}{\lambda_m \delta_n} \frac{(Q_2 Q_4 - Q_1 Q_3)}{Q_2^2 - Q_1^2} + 4A_{26}^* \frac{(Q_2 Q_3 - Q_1 Q_4)}{Q_2^2 - Q_1^2} + 4(B_{21}^* \lambda_m^2 + B_{22}^* \delta_n^2)$$

$$L_2 = \frac{\lambda_m^2}{8}, L_4 = \frac{\delta_n^2}{8}$$

$$H_1 = D_{11}^* \alpha_1 + D_{12}^* \alpha_2$$

$$H_2 = D_{12}^* \alpha_1 + D_{22}^* \alpha_2$$